



Green Synthesis of Bi^{3+} – Mg^{2+} Layered Doubled Hydroxides – MnO_2 Nanocomposites Supercapacitors

P. Vanitha^a, K. Karthikeyan^{b,} and A. Thirumoorthi^c*

^a Student, M. Sc. Chemistry, P. G. Department of Chemistry, Government Arts College, Udumalpet – 642 126, Tamilnadu, India.

^b Guest lecturer, P.G. Department of Chemistry, Government Arts College, Udumalpet – 642 126, Tamilnadu, India.

^c Assistant Professor, P.G. Department of Chemistry, Government Arts College, Udumalpet – 642 126, Tamilnadu, India.

ABSTRACT

The Bi^{3+} – Mg^{2+} intercalated MnO_2 LDH has been synthesized by approach using Citric acid chemical route and lemon peel extract green synthesis route. The reducing agents of citric acid and lemon peel extract effects on synthesis of MnO_2 in layered host of LDH has been investigated. The characterizations were done using by IR, UV-visible, XRD and SEM spectral studies. The electrochemical property in capacitance behaviour found using electrolytes 2M KOH solution 108 F g^{-1} at a scan rate of 10 mV s^{-1} for green synthesized MnO_2 intercalated Bi^{3+} – Mg^{2+} LDHs.

Keywords: LDHs, MnO_2 , Green synthesis, Capacitance

1. Introduction

The anionic clay type as Layered double hydroxides (LDHs), was denoted the general formula $[\text{M}^{2+}_{1-x}\text{M}^{3+}_x(\text{OH})_2](\text{A}^{n-})_x \cdot n\text{H}_2\text{O}$ where M^{2+} was a divalent cation (Mg^{2+} , Zn^{2+} , Cu^{2+} , Ni^{2+} , Co^{2+} etc.), M^{3+} was a trivalent cation (Al^{3+} , Fe^{3+} , Cr^{3+} etc.), A^{n-} was an interlayer anion (CO_3^{2-} , SO_4^{2-} , NO_3^- , Cl^- , OH^- , etc.), and x was the ratio of divalent to trivalent cations [1, 2]. LDHs have broad attentions since of their large specific surface area, memory effect, high chemical stability, adsorption property [3]. The A^{n-} anions, in the interlayer of the LDHs host layers, can be exchanged with other ones or species by using an intercalation reaction, many pillared LDHs materials with different morphology and property can be prepared, and the obtained pillared LDHs materials have been used for supercapacitor or lithium ion secondary batteries [4]. In general, supercapacitors include electrical double-layer capacitors (EDLCs) and pseudocapacitors based on the working principles. The energies in EDLCs are stored in the electric double-layer via electrostatic accumulation of charges while pseudocapacitors mainly utilize reversible Faradaic reactions to keep the energies, providing higher mass and/or volumetric specific capacitance [5– 8]. Normally, metal oxides (such as CoO_x , MnO_2 , and Fe_2O_3) [9 – 11] and conducting polymers (PPy, PANI, and PEDOT) are widely utilized pseudo capacitive electrode materials.

Manganese dioxide (MnO_2) has attracted great interest because of the variety of their structures and unique properties [12]. They find potential applications such as catalysts, solar cells and electrochemical capacitors, electrode materials of Li-ion and Li-air batteries [13-17] due to their low cost, earth abundance, environmental friendliness and variable oxidation states [18]. Liu et al. reported such a battery, the capacity of which was 285 $\text{mAh}\cdot\text{g}^{-1}$ (MnO_2), with capacity retention of 92% over 5000 cycles [19]. MnO_2 is thus a promising candidate to be the electrode of next generation of commercial

* Corresponding author. Tel.: 9360644240 ;

E-mail address: karthikathiravan2@gmail.com

rechargeable batteries. The next problem is thus to optimize the synthesis of this material in terms of cost and environmental friendliness.

Hongjuan Li et al. reported that Ni^{2+} - Fe^{3+} layered double hydroxides (LDHs)/ MnO_2 layered nanocomposite has been fabricated by using both layer-by-layer self-assembly method, Ni^{2+} - Fe^{3+} LDHs/ MnO_2 nanocomposite exhibits a relative good capacitive behavior in a neutral electrolyte system, and its initial capacitance value is 104 F g^{-1} [20]. Lianlian Liu et al. synthesized the MnO_2 nano sheets were directly deposited on the NiCo-LDH to form three-dimensional (3D) self-supported core-shell $\text{MnO}_2/\text{NiCo-LDH}/\text{CC}$ flexible electrodes and found capacitive performance of 312 F g^{-1} [21].

Qing Sun et al. [22] found NiFe-LDH@FeOOH nanocomposites present high specific capacitance (1195 F/g at a current density of 1 A/g), lower resistance and well cycling performance (90.36% retention after 1000 cycles). Besides, the NiFe-LDH@ MnO_2 /NiFe-LDH@FeOOH supercapacitor exhibits 22.68 Wh/kg energy density at 750 W/kg power density, demonstrating potential application in energy storage devices. Hao Luo et al. found Core-sheath hierarchical-architected materials $\text{MnO}_2@/\text{Co-Ni LDH}$ possesses highly micro-structural integrity and using as positive electrode for pseudocapacitor, this material exhibits large specific capacitance of 1436 F g^{-1} at a current density of 1 A g^{-1} .

Bismuth based materials [23] possess exclusive band structures and high photo-corrosion stability. The perovskite BiFeO_3 nanocrystalline thin film electrode exposed comparable specific capacitance of 81 Fg^{-1} and electrochemical supercapacitive performance and stability in an aqueous NaOH electrolyte to that of commonly used ruthenium based perovskites. The perovskite BiFeO_3 nanocrystalline electrode used for supercapacitor applications [24, 25].

In this study, we report MnO_2 intercalated Bi^{3+} - Mg^{2+} LDHs nanocomposites were synthesized by two methods one is chemical route using citric acid and another one is eco-friendly route lemon peel extract used as a reducing agent. The chosen of lemon peel since it has three reducing reagents flavanoid glycoside, p-coumaric acid and β - sitosterol. The effect of reducing agents on synthesize of Bi^{3+} - Mg^{2+} - MnO_2 LDHs nanocomposites and investigated their behavior of optical, crystalline size, morphology and capacitance. The as-prepared samples were characterized by FT-IR, UV, XRD, SEM, and Photoluminescence. The electrochemical properties of both samples were evaluated by cyclic voltammetry.

2 EXPERIMENTAL SECTION

2.1 Lemon peel extracts preparation

10 g of peel of lemon were successively washed, dried at 90°C , and boiled in distilled water for 10 min at 100°C . The peel extract was filtered.

2.2 Preparation of Bi^{3+} - Mg^{2+} LDHs

Equimolar ratio of $\text{Bi}(\text{NO}_3)_3 \cdot 9\text{H}_2\text{O}$ and $\text{Mg}(\text{NO}_3)_2 \cdot 6\text{H}_2\text{O}$ in a molar ratio dissolved in 100ml deionized water and added 1 M HNO_3 (2ml) stirred well for homogeneous mixture. The solution of metal nitrates was slowly poured into the solution NaOH solution maintained pH – 12 under vigorous stirring. After mixing, the obtained slurry was aged at 80°C for 6 h, filtered, washed with distilled water and dried in an oven at 60°C . Bi^{3+} - Mg^{2+} LDHs [BMLDHs] was attained [26].

2.3 Synthesize MnO_2 intercalated LDHs nanocomposites

LDHs material (2 g) was treated with 1.2 mol L^{-1} aqueous solution of KMnO_4 for 1 day at room temperature MnO_4 - LDHs material was obtained. The precipitate was isolated by filtration and washed several times with distilled water to remove potassium ions and dried 60°C . MnO_4 -LDHs obtained.

Then the MnO_4 -LDHs added with 50ml distilled water and then add 50ml peel extract after stirring vigorously for 5 h at room temperature this mixture changed in color from pale brown to dark brown due to reduction finally MnO_2 - LDHs synthesized. The collected precipitate was dried overnight at 60°C [27]. The sample has been given description as BMLDHM- LP.

In chemical route, MnO_2 - LDHs synthesized same manner described above however citric acid has been added as an alternative of lemon peel extract. The sample has been given description as BMLDHM- C.

3 RESULTS AND DISCUSSION

3.1 UV – VISIBLE

Hongjuan Li et al. found that multilayer growth of $(\text{Ni}^{2+}$ - Fe^{3+} LDHs/ MnO_2)_n is examined by recording the UV-vis absorption spectral studies. A broad absorption band centered at around 365 nm is characteristic of manganese oxide nanosheets. While the Ni^{2+} - Fe^{3+} LDHs nanosheets deposited on quartz slide show no optical absorption in the wavelength range of 200–800 nm. The absorbance at 365 nm increases almost nearly linear in proportion to the number of layer pairs, indicating the Ni^{2+} - Fe^{3+} LDHs nanosheets and MnO_2 nanosheets are successfully assembled [20].

In Fig. 1 shows UV- visible spectral of LDHM - C and LDHM - LP nanocomposites respectively. The peak found the region at 310 – 325 nm due to MnO_2 present in the layered host of LDHs. The absorbance LDHM - LP has been increased due to MnO_2 assembled well in the layered space of LDHs. Meanwhile, Bi^{3+} - Mg^{2+} LDHs has no optical absorption.

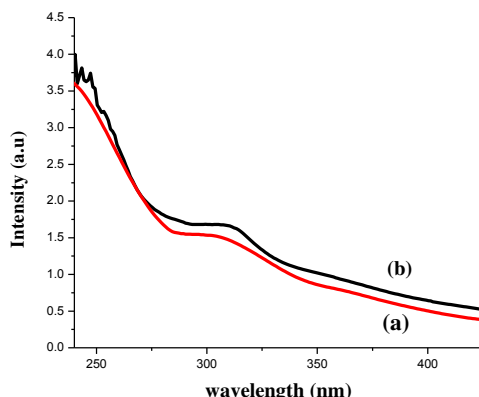


Fig. 1 – UV-visible spectra of synthesized nanocomposites (a) BMLDHM-C; (b) BMLDHM-LP.

Tauc’s plot

Energy band of materials is related to absorption coefficient α by the Tauc’s relation:

$$\alpha h\nu = A(h\nu - E_g)^n \dots\dots\dots (1)$$

Where A is a constant, $h\nu$ the photon energy, E_g the band gap and n is an index which assumes values 1/2, 3/2, 2 or 3 depending on the nature of the electronic transition responsible for the absorption. $n=1/2$ is taken for an allowed direct transition. Therefore, by plotting a graph between $(\alpha h\nu)^2$ and $h\nu$ in eV, a straight line is obtained which gives the value of the direct band gap. The extrapolation of straight line to $(\alpha h\nu)^2 = 0$ gives the value of the direct band gap of the material. Fig. 2 (a) and (b) shows that tauc’polt and found band gap 3.67 eV and 3.75 eV for synthesized BMLDHM-C and BMLDHM- LP nanocomposites respectively.

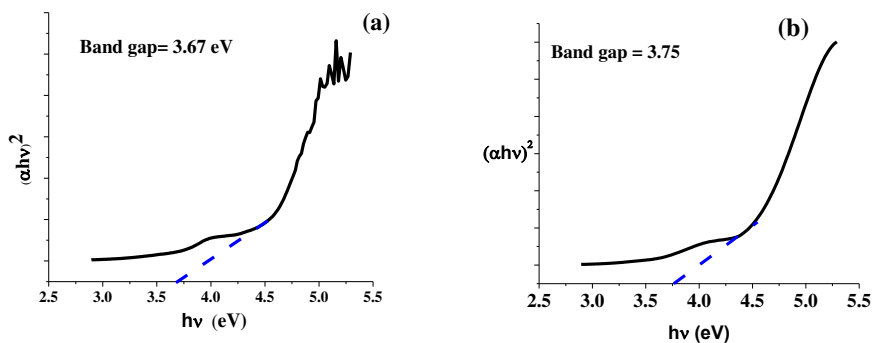


Fig. 2 – Tauc’s plot of synthesized nanocomposites (a) BMLDHM-C; (b) BMLDHM-LP.

3.2 XRD ANALYSIS

Zong – Huai Liu et al. suggested that MnO_2 pillared $Ni^{2+}-Fe^{3+}$ layered double hydroxides nanocomposite has been successfully fabricated using an intercalation/reduction reaction followed by heating treatment. The precursor, $Ni^{2+}-Fe^{3+}$ LDHs has a basal spacing of 0.78 nm and no peaks of impurities are discerned, indicating a high purity of the product. After intercalation of MnO_2 particles, the interlayer basal space increased to be 0.835 nm [28].

In Fig. 3 exposed that XRD pattern of layered doubled hydroxides with LDHM – C and LDHM – LP nanocomposites. The peaks at $2\theta = 11^\circ$ and 22° corresponding to the plane 003 and 006 respectively. The basal space of 003 plane of pure BMLDHS has been found $d=0.785$ further which was increased since intercalation of MnO_2 . That are confirmed by basal spaces of samples LDHM – C and LDHM – LP those are found $d=0.84$ and 0.88 respectively. Hence XRD pattern confirms the MnO_2 intercalated in the layer space of LDHs. The diffraction peaks assigned that rhombohedral structure of LDH meanwhile MnO_2 intercalated LDHs structure has been compared with pristine $Co^{2+}-Al^{3+}$ LDH (CALDH) [29]. Moreover, the basal reflection of BMLDHS-LP expanded, indicating the layer structure of the samples increased due to intercalation of MnO_2 .

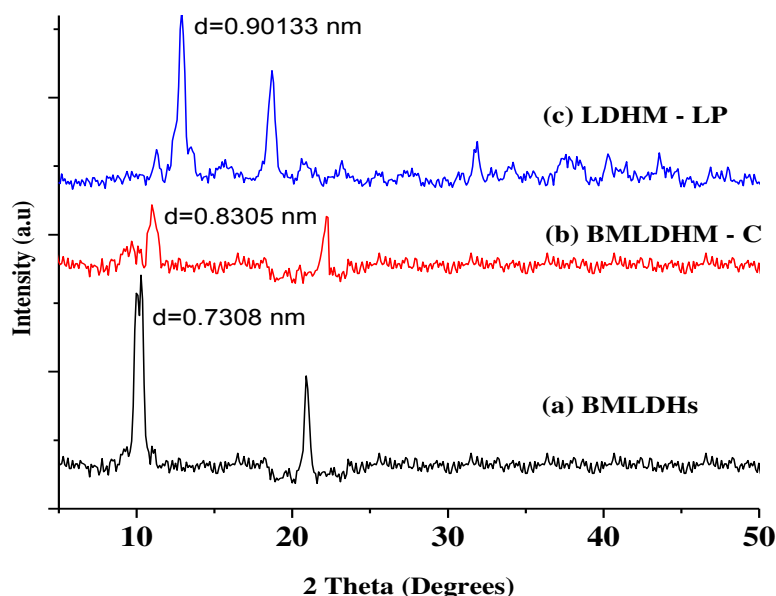


Fig. 3 – XRD spectra of synthesized nanocomposites (a) BMLDHs ; (b) BMLDHM-C ; (c) BMLDHM-LP.

Table 1 - Indexing of XRD patterns of synthesized nanocomposites.

Sample	d_{003} (nm)	d_{006} (nm)	d_{009} (nm)	d_{110} (nm)	Crystallite size in 'c' direction (nm)	Crystallite size in 'a' direction (nm)
CALDH	0.75264	0.37691	0.25126	0.15363	2.26023	0.30726
BMLDHs	0.73081	0.38225	0.24851	0.15077	2.24084	0.30154
BMLDH – C	0.83050	0.38616	0.24794	0.15037	2.41745	0.30074
BMLDH – LP	0.90133	0.39733	0.28123	0.15123	2.51886	0.30246

3.3 SEM analysis

Zhe Yan et al [30]. reported that MnO_2 -pillared Co^{2+} - Ni^{2+} - Fe^{3+} layered double hydroxide nanocomposite with porous structure has been successfully prepared by using an intercalation/reduction reaction and followed by heating treatment at 200°C . The precursor, LDHs material, is consisted of thin hexagonal platelets with a mean lateral size of about 300 nm. MnO_2 -LDHs material hexagonal platelet morphology was observed. Min Lia et al [31]. suggested that the flower-like Ni-Fe layered double hydroxides loaded on Ni foam (NF/NiFe LDHs) are synthesized via one-pot hydrothermal method. The SEM images of the sample picked at different growth time nanowire and flower like shape observed.

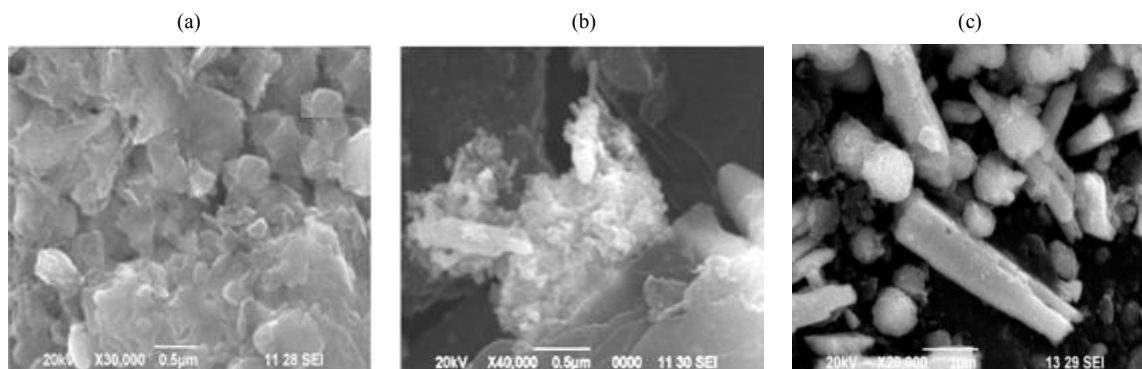


Fig. 4 – SEM morphology of synthesized nanocomposites (a) BMLDHs ; (b) BMLDHM-C; (c) BMLDHM-LP.

The Fig.4 shows that SEM images (a), (b) and (c) of BMLDHs, LDHM – C and LDHM – LP respectively. In Fig. 4 (a) shows SEM images of BMLDHs which observed platelet morphology mean while Fig. 5(b) LDHM – C exposed that irregular shape since intricate the growth of the MnO_2 nanoparticles formation during reduction, which explains the smaller size of the primary particles and size found to be 53nm. As shown in Fig. 4(c) LDHM-LP consists of fairly growth of nanorods and spherical shape of morphology observed an average size about 68 nm. It is clearly demonstrated that the nature of the reducing reagent in lemon peel has a strong effect on the morphology which support the growth of nanorods due to abundant phenolic compound p-coumarin acid, cholesterol similar structure β -sitosterol and flavonoid glycosides are anti-oxidative components in peel.

3.5 IR Spectral analysis

The broad band observed at 3458 cm^{-1} was attributed to O – H stretching modes of interlayer water molecules and H – bonded OH groups, and the peak at 1633 cm^{-1} corresponding to bending mode of water molecules. The bands in the range of $800 - 400\text{ cm}^{-1}$ were due to the Metal – Oxygen and Oxygen – Metal – Oxygen groups of lattice vibration bands. The LDHM – C and LDHM – LP shows a peak at 573 cm^{-1} indicates that the formation of the MnO_2 phase in the layered host. In Fig. 5 depicts the FT – IR spectra of BMLDHs, BMLDHM – C and BMLDHM – LP nanocomposites. It shows that peak of metal – oxygen bond $400 - 700\text{ cm}^{-1}$ besides interlayer water molecules peak intensity at the range of $1630 - 1640\text{ cm}^{-1}$ was decreased since MnO_2 intercalated into layered host of BMLDHs hence the peak was raised at $526 - 538$ corresponding to MnO_2 . The table 2 shows that the vibration peak position and assignment of the nanocomposites [32, 33].

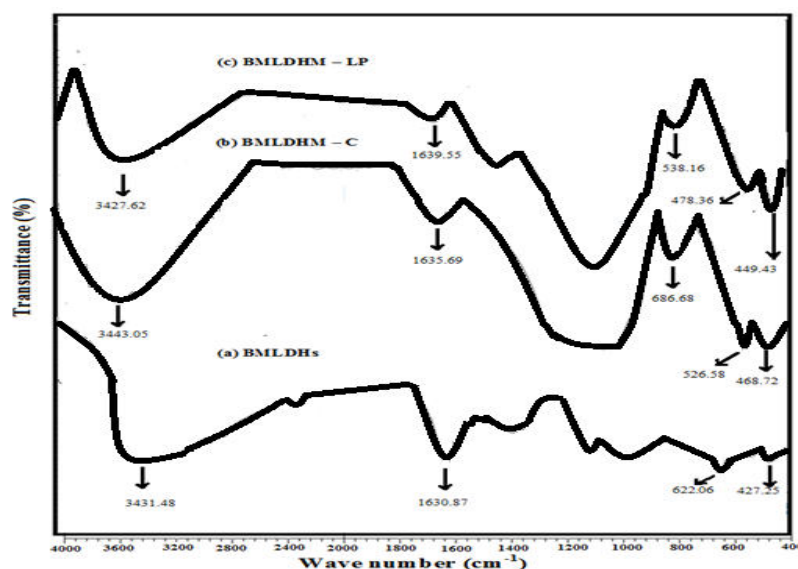


Fig. 5 – FT-IR spectra of synthesized nanocomposites (a) BMLDHs; (b) BMLDHM-C; (c) BMLDHM-LP.

Table 2 – FT-IR peak position and assignments comparison of synthesized nanocomposites.

Peak Positions (cm^{-1})			Assignments
BMLDHs	BMLDHM - C	BMLDHM – LP	
427.25, 622.06 and 664.50	468.72 and 686.68	449.43 and 478.36	Metal – Oxygen bonds (Bi – O, O – Mg / Bi – O)
–	526.58	538.16	MnO_2 Phase
1630.87	1635.69	1639.55	Bending mode of H_2O
3431.48	3443.05	3427.62	Interlayer O – H stretching modes

3. 4 CYCLIC VOLTAMMETRY

F. Li et al. synthesized low-cost high-performance asymmetric supercapacitors based on $Co_2AlO_4 - MnO_2$ nanosheets and Fe_3O_4 nanoflakes and suggested electrochemical properties of these composites displays a typical pseudocapacitive behavior with obvious redox peak clearly observed which can be assigned to the reaction of the Ni^{2+} / Ni^{3+} and Fe^{2+} / Fe^{3+} associated with OH^- . Besides, larger area of CV curves, showing much higher pseudocapacitance [34]. It derives from the extra pseudocapacitance from the contribution of the MnO_2 shell, which incorporates K^+ cations on the outer surface and/or possible intercalation and deintercalation of K^+ ions.

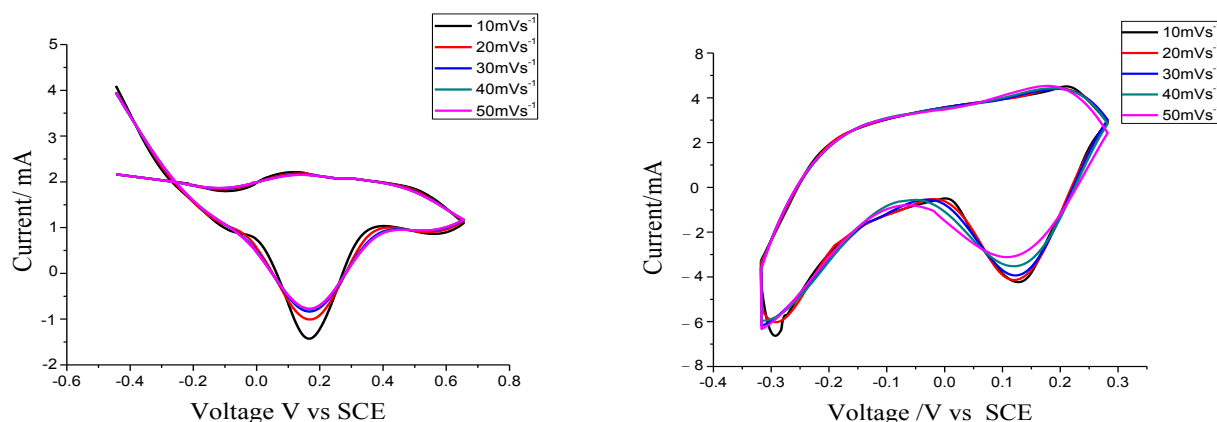


Fig. 6 – XRD spectra of synthesized nanocomposites (a) BMLDHM-C; (b) BMLDHM-LP.

The cyclic voltammograms (CVs) shown in Fig. 6. The discharge process broad current peak around 2.0 V. The cyclic voltammograms studies of LDHM – LP and LDHM – C have been investigated for their capacitance behavior in 2M KOH solution as the electrolyte at various scan rate 10mVs^{-1} – 50mVs^{-1} . The broadness of redox peaks is attributed to the poor crystallinity and morphology of MnO_2 in LDHM – C. The narrow peak was found at 1.5 eV for LDHM – LP since uniform growth MnO_2 with good crystalline in nature. The capacitance found sample LDHM – LP and LDHM – C has 108 Fg^{-1} and 62 Fg^{-1} respectively. The pseudocapacitive behavior apparent redox peak observed which can be confirmed to the reaction of the $\text{Bi}^{2+}/\text{Bi}^{3+}$ and $\text{Mg}^{2+}/\text{Mg}^{3+}$ reacted with hydroxyl ion in electrolyte. Besides, the better electrochemical performance of LDHM-LP is attributed due to crystalline nature and fair growth of MnO_2 in the layered host of BMLDHS.

4. Conclusions

The LDH intercalated MnO_2 synthesized (BMLDHS) successfully by using chemical route – citric acid (BMLDHM – C) and green synthesis – lemon peel (BMLDHM – LP). Both the crystallization and the electrochemical properties are enhanced in the BMLDHM – LP with respect to BMLDHM – C. This is ascribed to the fact that the lemon peel contains three reducing which leads to better results in the BMLDHM – LP. The IR spectral studies confirms that MnO_2 intercalated in the layered host of BMLDHS. UV –Visible spectra exposed that the intensity of peak of BMLDHM – LP is enhanced due to substantial intercalation. The XRD spectral studies show that the basal space of BMLDHS improved for BMLDHM – LP. SEM morphology found that lemon peel forms nanorods with spherical shape of crystalline MnO_2 which improves electrochemical properties of the BMLDHM – LP are as fine as those obtained with chemical reducing reagents. Moreover, using lemon peel has diminished both costly and polluting. This new way of synthesis of MnO_2 intercalated BMLDHS using for many applications in the industry, including electrochemical energy storage.

REFERENCES

1. Cavani, F., Trifirò, F., & Vaccari, A. (1991).Hydoalcite – type anionic clays: preparation, properties and applications. *Catalysis Today*, *11*, 173 – 301.
2. Duan, X., & Evans D.G. (2006). *Layered Double Hydroxides*, Springer, Verlag, Berlin Heidelberg.
3. Xuan, M.J., Shao, J.X., Dai, L., He, Q., Li, J.B. (2015). Macrophage cell membrane camouflaged mesoporous silica nanocapsules for in vivo cancer therapy, *Adv. Healthcare Mater.* *4* (11), 1645 – 1652.
4. Wang, Q., & O'Hare, D. (2012). Recent advances in the synthesis and application of layered double hydroxide (LDH) nanosheets, *Chem. Rev.*, *112*(7), 4124.
5. Yu, C., Yang, J., Zhao, C., Fan, X., Wang, G., & Qiu, J. (2014). Nanohybrids from NiCoAl – LDH coupled with carbon for pseudocapacitors: understanding the role of nanostructured carbon, *Nanoscale*, *6*, 3097–3104.
6. Xu, J., Gai, S., He, F., Niu, N., Gao, P., Chen, Y., & Yang, P. (2014). Reduced graphene oxide/ $\text{Ni}_{1-x}\text{Co}_x\text{Al}$ – layered double hydroxide composites: preparation and high supercapacitor performance, *Dalton Trans.*, *43*, 11667 – 11675.
7. Gupta, V., Gupta, S., & Miura, N. (2009). Electrochemically synthesized large area network of $\text{Co}_x\text{Ni}_y\text{Al}_z$ layered triple hydroxides nanosheets: a high performance supercapacitor, *J. Power Sources*, *189*, 1292 – 1295.
8. Zhang, L.J., Hui, K.N., San Hui, K., Lee, H.W. (2016). High-performance hybrid supercapacitor with 3D hierarchical porous flower-like layered double hydroxide grown on nickel foam as binder-free electrode, *J. Power Sources*, *318*, 76 – 85.
9. Zhai, T., Wan, L., Sun, S., Chen, Q., Sun, J., Xia, Q., & Xia, H. (2017). Phosphate ion functionalized Co_3O_4 ultrathin nanosheets with greatly improved

- surface reactivity for high performance pseudocapacitors, *Adv. Mater.*, 29, 1604167.
10. Jia, R., Zhu, F., Sun, S., Zhai, T., & Xia, H. (2017). Dual support ensuring high-energy supercapacitors via high-performance $\text{NiCo}_2\text{S}_4@\text{Fe}_2\text{O}_3$ anode and working potential enlarged MnO_2 cathode, *J. Power Sources*, 341, 427 – 434.
 11. Tang, X., Jia, R., Zhai, T., & Xia, (2015) H. Hierarchical $\text{Fe}_3\text{O}_4@\text{Fe}_2\text{O}_3$ core-shell nanorod arrays as high-performance anodes for asymmetric supercapacitors, *ACS Appl. Mater. Interfaces*, 7, 27518–27525.
 12. Wei, W., Cui, X., Chen, W., Ivey, D. G. (2011). Manganese oxide-based materials as electrochemical supercapacitor electrodes. *Chem. Soc. Rev.*, 40, 1697-1721.
 13. Debart, A., Paterson, A.J., Bao, J., Bruce, P.G. (2008). Alpha- MnO_2 nanowire: a catalyst for the O_2 electrode in rechargeable lithium batteries, *Angew Chem. Int. Ed.*, 47, 4521.
 14. Chou, S.L., Wang, J.Z., Chew, S.Y., Liu, H.K., & Dou, S.X. (2008). Electro deposition on MnO_2 nanowire on carbon nanotube paper as free –standing, flexible electrode for supercapacitors, *Electrochem. Commun.*, 10(11), 1724 – 1727.
 15. Lee, J., Lee, J.M., Yoon, S., Kim, S.O., Sohn, J.S., & Rhee, K.I. (2008). Electrochemical characteristics of manganese dioxide/carbon composites as a cathode material for Li/ MnO_2 secondary batteries, *J. Power Sources*, 183(1), 325 – 329.
 16. Sayle, T.X.T., Maphanga, R.R., Ngoepe, P.E., & Sayle, D.C. (2009). Predicting the electrochemical properties of MnO_2 nanomaterials used in rechargeable Li batteries : simulating nanostructure at the atomistic level, *J. Am. Chem. Soc.*, 131 (17), 6161 – 1673.
 17. Ida, S., Thapa, A.K., Hidaka, Y., Okamoto, Y., Matsuka, M., Hagiwara, H., & Ishihara, T. (2012). Manganese oxide with a card-house –like structure reassembled from nanosheets for rechargeable Li- air battery , *J. Power Sources*, 203, 159 – 164.
 18. Wang, Y., Ding, P., & Wang, C. (2016). Fabrication and lithium storage properties of MnO_2 hierarchical hollow cubes, *J. Alloys. Compd.*, 654, 273.
 19. Liu, T., Jiang, C., You, W., Yu, J. (2017). Hierarchical porous C/ MnO_2 composites hollow microspheres with enhanced supercapacitor performance, *J. Mater. Chem. A* 5 (18), 8635 – 8643.
 20. Hongjuan Li., Lingjuan Deng., Gang Zhu., Liping Kang., & Zong-Huai Liu. (2012). Fabrication and capacitance of $\text{Ni}^{2+}\text{-Fe}^{3+}$ LDHs / MnO_2 layered nanocomposites via an exfoliation/reassembling process, *Mat. Sci. and Eng., B.*, 177(1), 8 – 13.
 21. Lianlian Liu., Liang Fang., Fang Wu., Jia Hu., Shufang Zhang., Haijun Luo., Bashan Hu., & Miao Zhou. (2020). Self-supported core-shell heterostructure $\text{MnO}_2/\text{NiCo-LDH}$ composite for flexible high- performance super capacitor, *Journal of Alloys and Compounds*, 824, 153929.
 22. Qing Sun., Kexin Yao., Yuxin Zhang. (2020). MnO_2 - directed synthesis of $\text{NiFe-LDH}@\text{FeOOH}$ nanosheet arrays for supercapacitor negative electrode, *Chem. Lett.*, 31(9), 2343 -2346.
 23. Xi, J. J., Wang, H., Zhang, B.H., Zhao, F.Q., & Zeng, B.Z. (2020). Novel molecularly imprinted photoelectrochemical sensor for rutin based on $\text{Bi}_2\text{S}_3/\text{ZnIn}_2\text{S}_4$ hetero junction, *Sens. Actuat., B* 4, 128409.
 24. Lokhande, C.D., Gujar, T.P., Shinde, V.R., Mane, R.S., & Han Sung -Hwan. (2007). Electrochemical supercapacitor application of pevoskite thin films, *Electrochem. Commun.*, 9(7), 1805.
 25. Winter, M., Brodd, R., J. (2004). What are batteries , fuel cells, and supercapacitors?, *Chem. Rev.*, 104(10), 4245-4270.
 26. Chen, H.M., He, J.H., Zhang, C.B., He, H. (2007). Self-assembly of novel mesoporous manganese oxide nanostructure and their application in oxidative decomposition of formaldehyde, *J. Phys. Chem. C*, 111(49), 18033-18038.
 27. Hashem, A., Abuzeid, H., Kaus, M., Indris, S., Ehrenberg, H. (2018). Green synthesis of nanosized manganese dioxide as positive electrode for lithium-ion batteries using lemon juice and citrus peel, *Electrochimica Acta*, 262, 74-81.
 28. Hongjuan Li., Gang Zhu., Zupei Yang., Zenglin Wang., Zong-Huai Liu. (2010). *J. Colloid Interface Sci.*, 345, 228 – 233.
 29. Zeng Peng Diao., Yu Xin Zhang., Xiao Dong Hao., Zhong Quan Wen. (2014). Facile synthesis of $\text{CoAl-LDH}/\text{MnO}_2$ hierarchical nanocomposites for high-performance supercapacitors, *Ceramics International* 40, 2115 – 2120.
 30. Zhe Yan., Qiao Dang., Yue Lu., Zong-Huai Liu. (2017). Preparation and capacitance of MnO_2 pillared $\text{Co}^{2+}\text{-Ni}^{2+}\text{-Fe}^{3+}$ layered double hydroxide porous material supercapacitor, *Colloids and Surfaces A: Physicochem. Eng. Aspects* 520, 32–38.
 31. Min Lia., Ming Zhou., Zhong Quan Wen., Yu Xin Zhang. (2017)., flower like NiFe layered double hydroxides coated MnO_2 for high-performance flexible supercapacitors, *Journal of Energy Storage*, 11, 242 – 248.
 32. Z. Liu, R. Ma, M. Osada, N. Iyi, Y. Ebina, K. Takada, T. Sasaki. (2006). Synthesis, Anion Exchange, and delamination of Co-Al layered double Hydroxide: assembly of the exfoliates nanosheet/ polyanion composites films and magneto-optical studies, *Journal of the American Chemical Society*, 128 (14), 4872 – 4880.
 33. H. Peng, Y. Han, T. Liu, W.C. Tjiu, C. He. 2010. Morphology and thermal degradation behaviour of highly exfoliated CoAl -layered double hydroxide/polycaprolactone nanocomposites prepared by simple solution intercalation, *Thermochimica Acta* 502 (1-2), 1 – 7.
 34. Li, F., Chen, H., Liu, X.Y., Zhu S.J., Jia, J.Q., Xu C.H., Dong, F., Wen, Z.Q., Zhang, Y.X. (2016). Low-cost high-performance asymmetric supercapacitors based on $\text{Co}_2\text{AlO}_4@\text{MnO}_2$ nanosheets and Fe_3O_4 nanoflakes, *J. Mater. Chem. A*, 4, 2096 – 2104.